A CALCULATION OF THE ACOUSTIC SHEAR WAVE ATTENUATION IN SEA ICE

J. G. Hanse, et al

Washington University

Prepared for:

Coast Guard Research and Development Center

July 1974

N O T I C E

This document is disseminated under the sponsorship of the Department of Transportation in the interest of information exchange. The United States Government assumes no liability for its contents or use thereof.

The contents of this report reflect the views of the Applied Physics Laboratory, University of Washington, who is responsible for the facts and the accuracy of the data presented herein. The contents do not necessarily reflect the official views or policy of the Department of Transportation. This report does not constitute a standard, specification or regulation.

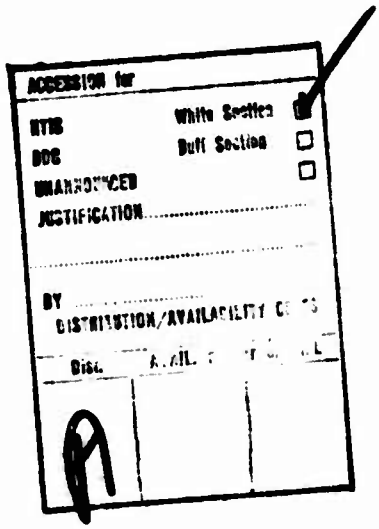

Technical Report Documentation Page

1. Report No.	2. Government Accession No.	3. Recipient's Catalog No.
CG-D-12-75		AD-786707

4. Title and Subtitle	5. Report Date
A CALCULATION OF THE ACOUSTIC SHEAR WAVE ATTENUATION IN SEA LIFE	July 1974
	6. Performing Organization Code
7. Author(s)	8. Performing Organization Report No.
J.G. Hanse and R.E. Bunney	APL-UW 7310
9. Performing Organization Name and Address	10. Work Unit No. (TRAIS)
Applied Physics Laboratory, University of Washington 1013 N.E. 40th Street Seattle, Washington 98195	751351
	11. Contract or Grant No.
	DOT-CG-24,595-A
12. Sponsoring Agency Name and Address	13. Type of Report and Period Covered
Department of Transportation U.S. Coast Guard Office of Research and Development Washington, D.C. 20590	Final Report
	14. Sponsoring Agency Code

15. Supplementary Notes

The contract under which this report was submitted was under the technical supervision of the Coast Guard Research and Development Center, Groton, Connecticut. R&D Center Report Number CGR&DC 21/74 has been assigned.

16. Abstract

The attenuation of an acoustic disturbance propagating in a medium which is not perfectly elastic, homogeneous and isotropic can be considered to be the result of energy dissipation due to classical processes and scattering. The contribution of each of these mechanisms is dependent upon the frequency of the sound wave. In this report several mathematical models are discussed for a transverse wave moving in a visco-elastic material and a scattering theory is developed. The theory is applied to sea ice and attenuation as a function of frequency is predicted for this material.

17. Key Words	18. Distribution Statement
Acoustic attenuation in sea ice Sea ice, acoustic attenuation in Transverse acoustic waves	Document is available to the public through the National Technical Information Service, Springfield, Virginia 22151

19. Security Classif. (of this report)	20. Security Classif. (of this page)	21. No. of Pages	22. Price
Unclassified	Unclassified		

Form DOT F 1700.7 (8-72) Reproduction of completed page authorized

CONTENTS

INTRODUCTION

Activities in much of the arctic region require a knowledge of ice thickness to assure safety of equipment and personnel. This knowledge is especially essential during exercises that require the operation of heavy equipment, for example, the employment of aircraft on ice runways for logistical support.

During the last 75 years, many studies of ice have been performed to understand its physical, mechanical and chemical properties. A thorough discussion of this work has been published by Weeks and Assur[1], so an extensive literature review will not be presented here. Even though some of these studies show ice to be a relatively good conductor of acoustic disturbances, an efficient method of acoustically determining ice thickness from the top surface still does not exist. Instead, ice thickness measurements are presently based on other physical characteristics of ice and water, such as dielectric permittivity, dielectric loss tangent in ice and in sea water, or elastic oscillations of the total ice cover.

Simple calculations based on the idealized assumption of isotropic, homogeneous ice indicate that, because of acoustic impedence matching at the ice-water interface, an incident acoustic compressional wave will be almost entirely transmitted into the water medium. Conversely, because the water will not support shear waves, the shear wave stress is assumed to vanish at the boundary. This assumption indicates that an acoustic shear wave impinging on the boundary will be reflected totally at normal incidence and less at greater angles. Thus, neglecting real and apparent attenuation, it would appear from this simple model that the best method of determining the ice thickness acoustically from the top surface would be to generate a shear wave in the ice and, knowing the wave speed, calculate the thickness from the reflection of the wave from the ice-water boundary.

It is known, however, that sea-ice is not a simple medium, but rather a highly complex inhomogeneous, anisotropic, polycrystalline material for which the acoustic propagation characteristics may be dependent on the growth and life history. Therefore, the ideal model discussed above is a gross oversimplification of the physics of the problem. One principal area of concern that must be resolved before ice thickness can be reliably measured with instrumentation based on shear wave propagation is the attenuation of the wave in the medium.

The attenuation of a sound wave propagating in a material that is not perfectly elastic, homogeneous and isotropic can be considered to be the result of two mechanisms which, for the purposes of this report, will be referred to as classical dissipation and scattering. Classical dissipation originates from many sources, a few of which are internal friction, anelastic behavior of the material, thermal dissipation, viscous slippage at crystal boundaries and the presence of dislocations and solute atoms in the medium. Energy losses

due to scattering originate from the interaction of the acoustic wave with scattering centers in the medium.

The relative contribution of each of these mechanisms to the total attenuation depends on the frequency of the sound wave. At low frequencies, the wavelength of the sound is very large compared to the scattering centers; therefore, the scattering cross section, i.e., the relative amount of energy scattered out of the incident wave, is extremely small and the attenuation is due almost entirely to classical dissipation. As the frequency increases, the attenuation due to scattering becomes more important until, when the wavelength becomes approximately on the order of the size of the scattering center, scattering eventually predominates.

We have performed a calculation of the attenuation from both classical dissipation and scattering which ultimately will allow the prediction of the total attenuation of a shear wave in sea ice. This report gives the results of that calculation and recommends that experiments be performed to evaluate the theories.

LONG WAVELENGTH ISOTROPIC SOLUTIONS

DERIVATION OF THE GENERAL EQUATIONS

For wavelengths that are long compared to the size of the scattering centers, i.e., at low frequencies, the calculation of acoustic velocity and attenuation can be derived ignoring the contributions due to scattering. Although all of the internal mechanisms contributing to classical dissipation are unknown, the general theory can be developed by grouping all attenuation sources as a simple constant. This is accomplished mathematically by the replacement of the shear modulus (M) and the Lame´ constant (Λ) in the elastic stress-strain relationships by the first order differential operators

$$\begin{aligned} M &= \mu + \mu' \frac{\partial}{\partial t} \\ \Lambda &= \lambda + \lambda' \frac{\partial}{\partial t} \end{aligned} \qquad (1)$$

In Eq. (1), the unprimed terms denote the elastic and the primed terms denote the viscous (or attenuative) contributions.

Consider an acoustic shear wave* moving in the positive (downward) x-direction. The displacement potential is given by

$$\psi = Ae^{i(\omega t - \alpha x)} , \tag{2}$$

where

ω is the circular frequency
t is the time
α is the complex wave number.

This displacement potential obeys the wave equation

$$\rho \frac{\partial^2 \psi}{\partial t^2} = M \nabla^2 \psi , \tag{3}$$

where ρ is the density of the medium and ∇^2 is the Laplacian operator. Substitution of Eqs. (1) and (2) into Eq. (3) yields

$$\rho \frac{\partial^2 \psi}{\partial t^2} = \mu \nabla^2 \psi + \mu' \nabla^2 \frac{\partial \psi}{\partial t} \tag{4}$$

or, carrying out the operations,

$$\rho \omega^2 = \alpha^2 (\mu + i\omega\mu') . \tag{5}$$

For a dissipative medium, the complex wave number can now be written as

$$\alpha = k - i\tau , \tag{6}$$

where

k is the running vector, ω/c
c is the wave velocity
τ is the generalized attenuation.

Thus, writing the potential in the form of Eq. (2),

$$\psi = Ae^{-\tau x} e^{i\omega(t - x/c)} , \tag{7}$$

*The derivation for the compressional wave propagation is similar to that presented here, the difference being the introduction of the (Λ + 2M) operator in the wave equation, Eq. (3), rather than the shear modulus (M) operator. The displacement potential must, of course, be associated with the compressional rather than the transverse wave.

which denotes a wave propagating in the positive x-direction with a velocity c and an amplitude which decays at a rate of τ per unit distance as the wave travels into the medium.

Making this substitution into Eq. (5) and separating the real and imaginary components yield the simultaneous equations

$$\begin{aligned} \rho\omega^2 &= \mu(k^2 - \tau^2) + 2\mu'\omega k\tau \\ 0 &= \omega\mu'(k^2 - \tau^2) - 2\mu k\tau \ . \end{aligned} \tag{8}$$

Setting

$$R = \frac{\mu'}{\mu} \ ,$$

these equations have the solutions

$$\begin{aligned} \tau &= \frac{k}{R\omega}\left\{\sqrt{1 + R^2\omega^2} \qquad -1\right\} \\ k^2 &= \frac{1}{2}\frac{\rho\omega^2}{\mu}\left\{\frac{\sqrt{1 + R^2\omega^2} \quad + 1}{1 + R^2\omega^2}\right\} \ , \end{aligned} \tag{9}$$

where now both μ and R may be frequency dependent. The procedure from this point is to introduce a mathematical model ot the medium composed of elastic and viscous constants which are frequency independent, and then fit the results to experimental data.

MATHEMATICAL MODELS OF VISCO-ELASTIC MATERIALS

Historically, there are many different rheological models that have been used to represent viscous materials. Although these models have been developed to interpret the results of static measurements, one or more of them can be applied to the results of dynamic tests, particularly if limited frequency ranges are being considered.

Maxwell Model

Consider the mechanical representation of a visco-elastic medium shown in Figure 1. Here, the material is represented by a spring denoting the elastic element (E_m) in series with a dash-pot denoting the viscous, or dissipative, element (η_m). In this model both E_m and η_m are frequency independent.

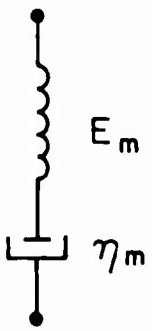

Figure 1. Maxwell's Mechanical Representation of Visco-Elastic Solids.

Maxwell[2] defined the stress-strain relationship for this visco-elastic solid as:

$$\frac{d}{dt}\sigma_{ij} = 2M\frac{d}{dt}S_{ij} - \frac{\sigma_{ij}}{\delta} \qquad (i \neq j) \ , \tag{10}$$

where σ_{ij} and S_{ij} are components of the stress tensor and the strain tensor, respectively, and δ is the relaxation time of the material. If the wave equation is to be applicable, Hooke's law states that the relationship between stress and strain must be of the form

$$\sigma = MS \ , \tag{11}$$

which, for this case, may be accomplished by writing the shear modulus (M) as an operator,

$$M = \frac{\mu}{1 + \frac{1}{\delta\frac{d}{dt}}} \ , \tag{12}$$

or, in terms of the elastic and viscous constants of Figure 1,

$$M = \frac{E_m}{1 + \frac{E_m}{\eta_m}\left(\frac{d}{dt}\right)^{-1}} \ . \tag{13}$$

Thus, substituting Eq. (13) into Eq. (11) and simplifying yield the relationship

$$\frac{d}{dt}\sigma_m + \frac{E_m}{\eta_m}\sigma_m = E_m\frac{d}{dt}S_m \ . \tag{14}$$

Now, for periodic stresses, both σ and S have time dependence of the form $e^{i\omega t}$. Equation (14) can then be reduced to

$$\sigma_m = \frac{E_m\omega^2 + i\omega \frac{E_m^2}{\eta_m}}{\left(\frac{E_m}{\eta_m}\right)^2 + \omega^2} S_m \ . \tag{15}$$

From the wave equation, Eq. (3), it was shown that the shear modulus operator (M) could be reduced to

$$M = \mu + i\omega\mu' \ . \tag{16}$$

Therefore, separating real and imaginary parts of Eq. (15) and comparing with Eq. (16),

$$\mu = \frac{E_m\omega^2}{\left(\frac{E_m}{\eta_m}\right)^2 + \omega^2}$$

$$\mu' = \frac{E_m^2/\eta_m}{\left(\frac{E_m}{\eta_m}\right)^2 + \omega^2} \tag{17}$$

so that

$$R\omega = \frac{\mu'}{\mu}\omega = \frac{E_m}{\eta_m\omega} \ . \tag{18}$$

The solution given by Eq. (9) can then be immediately written as

$$\tau = \frac{k\eta_m\omega}{E_m}\left\{\sqrt{1+\left(\frac{E_m}{\eta_m\omega}\right)^2} - 1\right\}$$

$$k^2 = \frac{\rho\omega^2}{2\mu}\left\{\frac{\sqrt{1+\left(\frac{E_m}{\eta_m\omega}\right)^2}+1}{1+\left(\frac{E_m}{\eta_m\omega}\right)^2}\right\}, \qquad (19)$$

which is the general solution for the Maxwell model of a visco-elastic solid. To evaluate the elastic and viscous constants, experiments must be performed to measure the acoustical velocity and attenuation at a given frequency. Equation (19), with the assistance of Eq. (17), represents two simultaneous equations with two unknowns so that the frequency-independent parameters E_m and η_m can be derived.

To determine the applicability of this model at high and low frequencies, consider the following. For $\omega >> E_m/\eta_m$,

$$\tau \approx k\left(\frac{\eta_m\omega}{E_m}\right)\left[1+\frac{1}{2}\left(\frac{E_m}{\eta_m\omega}\right)^2 - 1\right] \approx \frac{1}{2}\,k\,\frac{E_m}{\eta_m\omega} \qquad (20)$$

and

$$k^2 \approx \frac{\rho\omega^2}{2\mu}\,\frac{2+\frac{1}{2}\left(\frac{E_m}{\eta_m\omega}\right)^2}{1+\left(\frac{E_m}{\eta_m\omega}\right)^2} \approx \frac{\rho\omega^2}{\mu} \quad . \qquad (21)$$

But, from Eq. (17),

$$\mu = \frac{E_m}{1+\left(\frac{E_m}{\eta_m\omega}\right)^2} \approx E_m \quad . \qquad (22)$$

Therefore

$$k \approx \omega \sqrt{\frac{\rho}{E_m}} = \frac{\omega}{c} \quad , \tag{23}$$

which is the solution for an acoustic wave moving in an elastic medium. Therefore, for this model the medium appears to be elastic for velocity considerations. The attenuation is then given by

$$\tau \approx \frac{1}{c} \frac{E_m}{\eta_m} \approx \frac{\rho c}{\eta_m} \approx \text{constant} \quad . \tag{24}$$

For the low frequency case,

$$\omega << \frac{E_m}{\eta_m}$$

and

$$\tau \simeq k \tag{25}$$

but

$$k^2 \approx \frac{\rho\omega^2}{2\mu} \frac{\eta_m \omega}{E_m} \tag{26}$$

and

$$\mu \approx \frac{\eta_m{}^2 \omega^2}{E_m} \tag{27}$$

so

$$\tau \simeq k \approx \frac{\rho}{2\eta_m} \sqrt{\omega} \quad . \tag{28}$$

Thus at low frequencies both the attenuation and the velocity of the acoustic disturbance have frequency dependence of the form $\sqrt{\omega}$.

Voigt Model

Figure 2 shows the mechanical representation of a visco-elastic solid proposed by Voigt[3]. In this configuration, a spring with elasticity (E_V) is in parallel with a dashpot which represents the viscosity (η_V). As in the previous model, both E_V and η_V are assumed to be frequency independent.

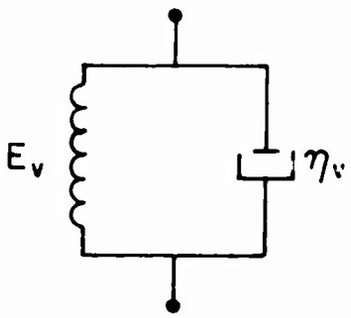

Figure 2. Voigt's Mechanical Representation of Visco-Elastic Solids.

The stress-strain relationship is given by

$$\sigma_v = \left(E_v + \eta_v \frac{d}{dt}\right) S_v \ . \tag{29}$$

Using techniques and arguments identical to those for the Maxwell model, it can be shown that the solutions for the Voigt model are given by the equation

$$\tau = \frac{kE_v}{\eta_v \omega}\left\{\sqrt{1 + \left(\frac{\eta_v}{E_v}\omega\right)^2} - 1\right\}$$

$$k^2 = \frac{1}{2}\frac{\rho\omega^2}{E_v}\left\{\frac{\sqrt{1 + \left(\frac{\eta_v}{E_v}\omega\right)^2} + 1}{1 + \left(\frac{\eta_v}{E_v}\omega\right)^2}\right\} . \tag{30}$$

where, for this case,

$$\mu = E_v$$

and (31)

$$\mu' = \eta_v$$

For the high frequency case, i.e., where $E_v/\eta_v\omega$ is small,

$$\tau \approx k$$

$$k \approx \sqrt{\frac{1}{2}\frac{\rho}{\eta_v}}\sqrt{\omega} \quad , \tag{32}$$

which is the same form as the low frequency limit of the Maxwell model, for which both the attenuation and the velocity vary with frequency as $\sqrt{\omega}$.

For the low frequency case, where $E_v/\eta_v\omega$ is large, the equations approximate to

$$\tau \approx \frac{1}{2} k \frac{\eta_v}{E_v} \omega \tag{33}$$

$$k^2 \approx \frac{\rho\omega^2}{E_v}$$

so that

$$k \approx \omega\sqrt{\frac{\rho}{E_v}}$$

$$\tau \approx \frac{1}{2}\sqrt{\frac{\rho\eta_v^2}{E_v^3}}\,\omega^2 \, . \tag{34}$$

This equation states that the velocity remains constant while the attenuation varies as the square of the frequency.

EXPANSION TO MORE COMPLEX MODELS

Very few solids behave even approximately like either the Maxwell or the Voigt model. However, since more complicated models become extremely involved mathematically and, further, since models specifying more parameters require more experimental evidence to substantiate or "fit" the models, using a single Maxwell or Voigt element is often a convenient method of obtaining a description of a visco-elastic solid's mechanical properties when its dynamic behavior is required for only a restricted region of frequencies.

For most materials, the use of single elements, although mathematically more desirable, must include the assumption that the elastic and viscous coefficients are frequency dependent. To eliminate this frequency dependence, a more complex model becomes necessary. The method used to construct a more

complex model is to build up various combinations of Voigt and Maxwell elements in series and parallel until the frequency dependence of the constants is removed.

As a example, consider the model shown in Figure 3, which consists of a Maxwell and a Voigt model in series. The stress-strain relationship for this configuration must be reduced to that described by Hook's law, which is given in Eq. (11). From earlier arguments, it has been shown that the Maxwell and Voigt elements of this model obey the equations

$$\frac{d}{dt}\sigma_m + \frac{E_m}{\eta_m}\sigma_m = E_m \frac{d}{dt} S_m \tag{14}$$

and

$$\sigma_v = (E_v + \eta_v \frac{d}{dt})\ S_v\ , \tag{29}$$

respectively.

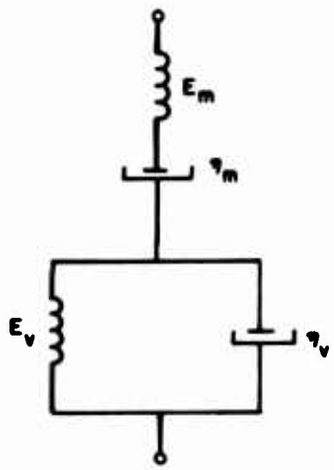

Figure 3. Mechanical Representation of the 4-Element Model.

To combine the elements, it must be recognized that the stress across the model is equally divided between the elements, whereas the strain is the sum of the extension of each element. Mathematically,

$$\begin{aligned} \sigma &= \sigma_v = \sigma_m \\ S &= S_v + S_m \end{aligned} \tag{35}$$

so, from Eqs. (10) and (29),

$$\frac{d}{dt}\sigma + \frac{E_m}{\eta_m}\sigma = E_m \frac{d}{dt} S_m \tag{36a}$$

$$\sigma = E_v S_v + \eta_v \frac{d}{dt} S_v \quad . \tag{36b}$$

The $e^{i\omega t}$ dependence cannot be substituted directly into Eq. (36) because each element may oscillate at frequencies which are quite different from the driving frequency. Thus, before the time dependence can be considered, the generalized Hooke's law for this case must be derived. Rewriting Eq. (36b) as

$$\frac{E_m}{\eta_v}\sigma = \frac{E_m E_v}{\eta_v} S_v + E_m \frac{d}{dt} S_v \tag{37}$$

and adding it to Eq. (36a) give

$$\frac{d}{dt}\sigma + \left(\frac{E_m}{\eta_m} + \frac{E_m}{\eta_v}\right)\sigma = \frac{E_m E_v}{\eta_v}(S - S_m) + E_m \frac{d}{dt} S \quad . \tag{38}$$

Differentiating Eq. (38) with respect to time gives

$$\frac{d^2}{dt^2}\sigma + \left(\frac{E_m}{\eta_m} + \frac{E_v}{\eta_v}\right)\frac{d}{dt}\sigma = \frac{E_m E_v}{\eta_v}\frac{d}{dt}(S - S_m) + E_m \frac{d^2}{dt^2} S \quad . \tag{39}$$

Solving Eq. (36a) for $(d/dt)S_m$, substituting into Eq. (39), and collecting terms yield the relationship between the time derivatives of the stress and total strain.

$$\frac{d^2}{dt^2}\sigma + \left(\frac{E_m}{\eta_m} + \frac{E_v}{\eta_v} + \frac{E_m}{\eta_v}\right)\frac{d}{dt}\sigma + \frac{E_m E_v}{\eta_m \eta_v}\sigma = E_m \frac{d^2}{dt^2} S + \frac{E_m E_v}{\eta_v}\frac{d}{dt} S \quad . \tag{40}$$

Now, for periodic driving forces,

$$\begin{aligned} \sigma &= \sigma_o\, e^{i\omega t} \\ S &= S_o\, e^{i\omega t} \quad . \end{aligned} \tag{41}$$

Substituting Eq. (41) into Eq. (40) and simplifying yield

$$\sigma_o = \left\{ \left[\frac{\omega^4 E_m + \omega^2 (E_m + E_v) \dfrac{E_m E_v}{\eta_v}}{\left(\omega^2 - \dfrac{E_m E_v}{\eta_m \eta_v}\right)^2 + \left(\dfrac{E_m}{\eta_m} + \dfrac{E_v}{\eta_v} + \dfrac{E_m}{\eta_v}\right)^2} \right] \right.$$

$$\left. + i\omega \left[\frac{\omega^2 E_m{}^2 \left(\dfrac{1}{\eta_m} + \dfrac{1}{\eta_v}\right) + \dfrac{(E_m E_v)^2}{\eta_m \eta_v{}^2}}{\left(\omega^2 - \dfrac{E_m E_v}{\eta_m \eta_v}\right)^2 + \left(\dfrac{E_m}{\eta_m} + \dfrac{E_v}{\eta_v} + \dfrac{E_m}{\eta_v}\right)^2} \right] \right\} S_o \qquad (42)$$

$$= MS_o \quad .$$

But, now

$$M = \mu + i\omega\mu'$$

so that

$$R\omega = \omega \frac{\mu'}{\mu}$$

$$= \frac{E_m}{\omega\eta_m} \frac{\left(1 + \dfrac{\eta_m}{\eta_v}\right) + \left(\dfrac{E_v}{\omega\eta_v}\right)^2}{1 + \left(1 + \dfrac{E_m}{E_v}\right)\left(\dfrac{E_v}{\omega\eta_v}\right)^2} \qquad (43)$$

where

$$\mu = \frac{E_m + \dfrac{1}{\omega^2}(E_m + E_v)\dfrac{E_m E_v}{\eta_v{}^2}}{\left(1 + \dfrac{1}{\omega^2}\dfrac{E_m E_v}{\eta_m \eta_v}\right)^2 + \dfrac{1}{\omega^2}\left(\dfrac{E_m}{\eta_m} + \dfrac{E_v}{\eta_v} + \dfrac{E_m}{\eta_v}\right)^2} \quad . \qquad (44)$$

To investigate the behavior of this model, the asymptotic frequency limits must be examined. For high frequency,

$$\lim_{\omega \to \text{large}} (\mu) = E_m$$

$$\lim_{\omega \to \text{large}} (R\omega) = \frac{E_m}{\omega \eta_m}\left(1 + \frac{\eta_m}{\eta_v}\right)$$

$$\lim_{\omega \to \text{large}} (\tau) = \frac{1}{2} k R\omega \tag{45}$$

but,

$$\lim_{\omega \to \text{large}} (k) = \frac{\rho}{E_m} \tag{46}$$

so that

$$\lim_{\omega \to \text{large}} (\tau) = \frac{1}{2}\sqrt{\frac{\rho}{2E_m}}\ \frac{E_m}{\eta_m}\left(1 + \frac{\eta_m}{\eta_v}\right) = \text{constant} , \tag{47}$$

and, for low frequency,

$$\lim_{\omega \to \text{small}} (\mu) = \text{const} \times \omega^2$$

$$\lim_{\omega \to \text{small}} (R\omega) = \frac{E_m}{\omega \eta_m}\ \frac{1}{\left(1 + \frac{F_m}{\eta_v}\right)} \tag{48}$$

$$\lim_{\omega \to \text{small}} (\tau) = k$$

$$\lim_{\omega \to \text{small}} (k) = \text{const} \times \sqrt{\omega} \quad . \tag{49}$$

Comparison of Eqs. (46), (47) and (49) with the asymptotic limit solutions of the Maxwell model shows that both models have the same form of frequency dependence in the limit of both the high and low frequencies. Therefore, the Maxwell element predominates the frequency dependence of this model. The limits, of course, are different because the coefficients are highly modulated by the Voigt element.

EXTENSION OF THE THEORY TO INCLUDE ANISOTROPY

Thus far in the theory, only the solutions for an isotropic medium have been discussed. It is known, however, that for many materials, including naturally occurring ice, the acoustic properties exhibit a dependence on the direction of the propagation of the wave relative to the crystal axis, i.e., the media are not isotropic. A method of including anisotropy in the theory follows.

Stresses and strains in the medium can be specified in terms of the resolved displacements in a unit cube of the material.[4] There are six components of stress and six of strain which can be written in terms of tensor notation as

$$\sigma_{ij} \text{ and } S_{ij} \ ,$$

where i,j denote the x-, y-, z- or 1-, 2-, 3-component of the stress or strain. The force of a unit cube in the i^{th} direction is given by

$$F_i = \frac{\partial \sigma_{ij}}{\partial x_j} \, dxdydz \ , \tag{50}$$

where repeated indices indicate a summation. The tensor strains are defined by

$$S_{ij} = \frac{1}{2}\left(\frac{\partial u_i}{\partial x_j} + \frac{\partial u_j}{\partial x_i}\right) \ , \qquad i,j = 1,2,3 \ , \tag{51}$$

where the u_j's are the displacements of the body along the coordinate direction x_j.

Utilizing the reduced tensor convention for the stresses

$$\begin{aligned} &\sigma_1 = \sigma_{11}; \ \sigma_2 = \sigma_{22}; \ \sigma_3 = \sigma_{33} \\ &\sigma_4 = \sigma_{23} = \sigma_{32}; \ \sigma_5 = \sigma_{13} = \sigma_{31}; \ \sigma_6 = \sigma_{12} = \sigma_{21} \ , \end{aligned} \tag{52}$$

and, similarly, for the strains

$$\begin{aligned} &S_1 = S_{11}; \ S_2 = S_{22}; \ S_3 = S_{33} \\ &\frac{S_4}{2} = S_{23} = S_{32}; \ \frac{S_5}{2} = S_{13} = S_{31}; \ \frac{S_6}{2} = S_{12} = S_{21} \ , \end{aligned} \tag{53}$$

the generalized Hooke's law may then be written

$$\sigma_i = c_{ij} S_j \qquad i,j = 1,2\ldots,6 \quad , \tag{54}$$

and it can be shown that for the elastic constants

$$c_{ij} = c_{ji} \tag{55}$$

there are a maximum of 21 elastic constants for the most unsymmetrical crystal. As the degree of symmetry increases the number of elastic constants decreases until there are only two for an isotropic medium. These are the Lame´ constants λ and μ, where

$$\begin{aligned} \lambda + 2\mu &= C_{11} = C_{22} = C_{33} \ , \\ \lambda &= C_{12} = C_{13} = C_{23} = C_{21} = C_{31} = C_{32} \ , \\ \mu &= C_{44} = C_{55} = C_{66} \ , \end{aligned} \tag{56}$$

and all other constants are zero.

To include anisotropy in the theories developed in this report, each of the elastic constants is replaced by a differential operator of the proper form for the model being considered. Therefore, a complete solution will require the determination of two or more elastic and viscous constants for each operator used.

SHORT WAVELENGTH SOLUTIONS

GENERAL DISCUSSION

An acoustic wave propagating in a nonhomogeneous medium will interact with the inhomogeneities to scatter part of the energy out of the sound beam. When the wavelength of the sound is large compared to the size of these scattering centers, the interaction is minimal and the energy loss is small compared to that caused by classical dissipation. For this situation, the acoustic attenuation can be predicted by the long wavelength theories discussed in the previous section. However, when the size of the scattering center is a significant portion of a wavelength, the contribution to the attenuation due to scattering processes cannot be neglected.

To determine the attenuation due to scattering, consider an isotropic solid elastic medium containing a concentration of scatterers. The inhomogeneities in the medium can be mathematically characterized by a generalized function,

$$D(S,I,a,\vec{r}\ldots) = S(s_i)I(s_i,s_j)G(a,\vec{r})\ldots \ , \tag{57}$$

where $S(s_j)$ is a structure distribution function which describes the relative importance of the various types of scatterers in the medium, $I(s_i,s_j)$ is a distribution function which describes the interaction between scatterers and multiple scattering of the sound, and $G(a,\vec{r})$ describes the distribution of the size and position, etc. of the scatterers.

Assuming a plane wave moving in the positive x-direction, the intensity of the sound is given by

$$I = I_o\, e^{-2\alpha x} \ , \tag{58}$$

where α is the attenuation constant, x is the penetration distance into the material and I_o is the intensity of the original sound wave. If the energy losses are all considered to be due to scattering processes, Eq. (58) may be rewritten

$$I = I_o\, e^{-\Gamma x} \ , \tag{59}$$

where Γ is the generalized scattering cross section and is governed by the size, shape, position, etc. of the scatterers in the medium. In terms of Eq. (57), Γ may be written

$$\Gamma = \sum_{i,j} \int_{\vec{r}} \int_{a} \ldots D(S,I,G,\vec{r},\ldots)\ \gamma_i(a)\,d\vec{r}\,da\ldots \ , \tag{60}$$

where now $\gamma_i(a)$ is the scattering cross section of a single independent scatterer. The attenuation is then given by

$$\alpha = \frac{1}{2}\sum_{ij} \int_{\vec{r}} \int_{a} \ldots D(S,I,G,\vec{r},\ldots)\ \gamma_i(a)\,d\vec{r}\,da\ldots \ . \tag{61}$$

This equation states that the attenuation is determined by the scattering cross section and the distribution of the scatterers. The cross section is dependent upon the interaction of the wave with each individual scatterer while the distribution function is the probability of the wave encountering that scatterer in the medium.

SCATTERING OF A PLANE WAVE FROM A SPHERICAL OBSTACLE

Consider the problem shown in Figure 4. An acoustic plane wave propagating in an isotropic elastic solid encounters a spherical scatterer which, for present discussion, is also assumed to be elastic. Both media are characterized by their

densities (ρ_i), shear moduli (μ_i) and Lame´ constants (λ_i). Elasticity theory defines the compressional and transverse velocities as

$$C_{L_i} = \sqrt{\frac{\lambda_i + 2\mu_i}{\rho_i}} = \frac{\omega}{k_i}$$

$$C_{T_i} = \sqrt{\frac{\mu_i}{\rho_i}} = \frac{\omega}{K_i} \qquad (62)$$

respectively, where ω is the circular frequency and k_i and K_i are the wavenumbers. The displacement ($\vec{u}$) can be written in terms of the displacement potentials ϕ and ψ as

$$\vec{u} = \text{grad}\ \phi + \text{curl}\ \vec{\psi} \ . \qquad (63)$$

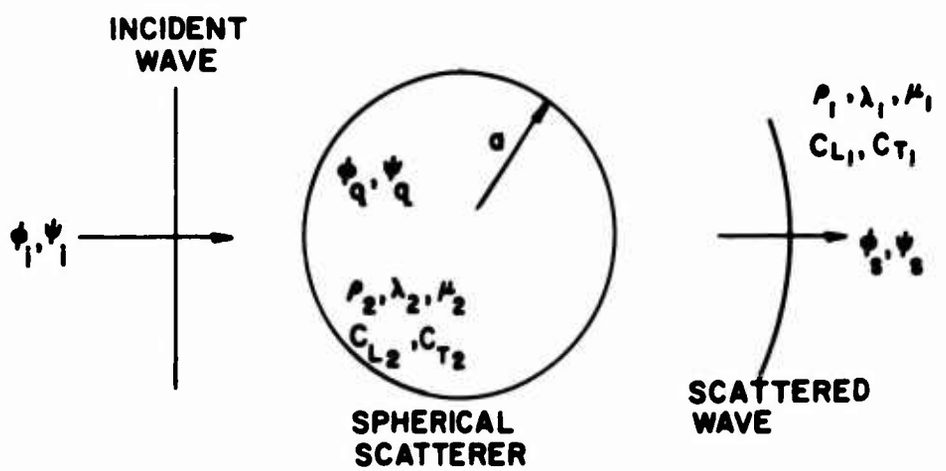

Figure 4. Representation of the Problem.

In spherical coordinates,

$$\vec{u} = -\nabla\phi + \nabla x \nabla x (\vec{r}\psi) \ , \qquad (64)$$

which is valid for spherically symmetric waves. The displacement potentials in spherical coordinates are of the form

$$\sum_{m=0}^{\infty} C_m f_m(pr)\ P_m(\cos\theta)\ e^{i\omega t} \ , \qquad (65)$$

and must obey the wave equations

$$\nabla^2\phi = \frac{1}{C_L^2}\frac{\partial^2\phi}{\partial t^2}$$

$$\nabla^2\psi = \frac{1}{C_T^2}\frac{\partial^2\psi}{\partial t^2} \tag{66}$$

where

$f_m(pr)$ = the spherical Bessel function of order m

p = either k or K, depending upon the wave considered

$P_m(\cos\theta)$ = the Legendre polynomial of order m.

When the incident plane wave strikes the scattering center, some of the energy is scattered away and some is transmitted through the scatterer. Since all the waves must obey the same wave equations, the wave potentials, neglecting the time dependence, may be written as

$$\phi \text{ Incident} = \sum_{m=0}^{\infty} I_{cm}\, j_m(k_1 r)\, P_m(\cos\theta)$$

$$\psi \text{ Incident} = \sum_{m=0}^{\infty} I_{sm}\, j_m(K_1 r)\, P_m(\cos\theta) \tag{67}$$

$$\phi \text{ Scattered} = \sum_{m=0}^{\infty} A_m\, h_m(k_1 r)\, P_m(\cos\theta)$$

$$\psi \text{ Scattered} = \sum_{m=0}^{\infty} B_m\, h_m(K_1 r)\, P_m(\cos\theta)\ , \tag{68}$$

$$\phi \text{ Transmitted} = \sum_{m=0}^{\infty} C_m\, j_m(k_2 r)\, P_m(\cos\theta)$$

$$\psi \text{ Transmitted} = \sum_{m=0}^{\infty} D_m\, j_m(K_2 r)\, P_m(\cos\theta) \tag{69}$$

where r and θ are spherical coordinates. The spherical Bessel functions of the first kind, $j_m(kr)$, and third kind, $h_m(kr)$, are used to assure that the scattered wave is propagating away from the scatterer located at the origin of the coordinate system. In order for the incident wave to be plane and of unit amplitude, I_{cm} and I_{sm} must be of the form[5]

$$I_m = \frac{(-i)^{m+1}}{p} (2m + 1) \ , \tag{70}$$

where p is k and K, respectively. The coefficients A_m, B_m, C_m and D_m are determined by the boundary conditions at the scattering surface. For a solid-solid interface with no slippage these boundary conditions are

(a) Radial displacement continuous
(b) Tangential displacement continuous
(c) Radial stress continuous
(d) Tangential stress continuous.

(When the scattering sphere is fluid filled, slippage is allowed and the requirement that the tangential displacement be continuous is no longer valid.) At the boundary, r = a, these conditions can be written mathematically as

$$\begin{aligned}
&\text{(a)} \quad u_{r(inc)} + u_{r(scatt)} = u_{r(trans)} \\
&\text{(b)} \quad u_{\theta(inc)} + u_{\theta(scatt)} = u_{\theta(trans)} \\
&\text{(c)} \quad \sigma_{rr(inc)} + \sigma_{rr(scatt)} = \sigma_{rr(trans)} \\
&\text{(d)} \quad \sigma_{\theta r(inc)} + \sigma_{r\theta(scatt)} = \sigma_{r\theta(trans)} \ .
\end{aligned} \tag{71}$$

In terms of the displacement potentials, the stress and displacement components of Eq. (71) are[6]

$$\begin{aligned}
\sigma_{rr} &= \rho\omega^2 \left\{ \phi + \frac{2}{K^2} \left[\frac{2}{r} \frac{\partial\phi}{\partial r} + \frac{1}{r^2} \Omega\phi - \frac{\partial}{\partial r} \left(\frac{1}{r} \Omega \psi \right) \right] \right\} \\
\sigma_{\theta r} &= -2 \frac{\rho\omega^2}{K^2} \frac{\partial}{\partial\theta} \left[\frac{1}{r} \frac{\partial\phi}{\partial r} - \frac{1}{r^2} \phi + \frac{1}{r} \frac{\partial\psi}{\partial r} + \frac{1}{r^2} \left(1 + \frac{K^2 r^2}{2} \right) \psi + \frac{1}{r^2} \Omega \psi \right] , \\
u_r &= - \left[\frac{\partial\phi}{\partial r} + \frac{1}{r} \Omega \psi \right] \\
u_\theta &= - \frac{1}{r} \frac{\partial\phi}{\partial\theta} + \frac{1}{r} \frac{\partial^2}{\partial r \partial\theta} (r\psi)
\end{aligned} \tag{72}$$

where

$$\Omega = \frac{1}{\sin\theta}\frac{\partial}{\partial\theta}\left(\sin\theta\,\frac{\partial}{\partial\theta}\right) \quad . \tag{73}$$

The scattering cross section is determined by calculating the ratio of the time rate at which energy is scattered out of the wave by an obstacle of radius "a" to the total energy of the incident wave. The scattered energy is equal to the energy being carried away by the scattered wave across a spherical surface of radius "b" > "a". Love[4] gives this scattered energy as

$$E_{\text{scattered}} = \iint_A \left\{ \sigma_{xr}\frac{\partial u_x}{\partial t} + \sigma_{yr}\frac{\partial u_y}{\partial t} + \sigma_{zr}\frac{\partial u_z}{\partial t} \right\}_{\text{scattered}} dA \quad , \tag{74}$$

where σ_{xr}, σ_{yr} and σ_{zr} are the stress components acting in the three rectangular axes on a surface normal to the radius vector $\vec{r}$, and the u's are displacements. Both the σ's and the u's are generally complex, so care must be exercised to assure that the final expression for the scattered energy is real. Assuming a time dependence of $e^{i\omega t}$ for the displacement potentials and using the spherical symmetry of the scattered wave, Eq. (74) can be rewritten in spherical coordinates as

$$E_{\text{scattered}} = \frac{i\omega}{2}\int_0^{\pi} \left\{ \left[\sigma_{rr} u_r^* + \sigma_{\theta r} u_\theta^* + \sigma_{zr} u_z^* \right] \right.$$

$$\left. - \left[\sigma_{rr}^* u_r + \sigma_{\theta r}^* u_\theta + \sigma_{zr}^* u_z \right] \right\}_{\substack{r=b \\ \text{scattered} \\ \text{wave}}} 2\pi b^2 \sin\theta d\theta \quad , \tag{75}$$

where all the terms are defined by Eq. (72) and the asterisk denotes the complex conjugate. The integral in this equation can be evaluated by substituting Eqs. (68) and (72) and using the identity which is valid for any two arbitrary functions f and g,

$$\int_0^{\pi} (\Omega f)\, g \sin\theta d\theta = \int_0^{\pi} f(\Omega g) \sin\theta d\theta = -\int_0^{\pi} \frac{\partial f}{\partial\theta}\frac{\partial g}{\partial\theta}\sin\theta d\theta \quad , \tag{76}$$

to determine the recursion relations and the orthogonality of the Bessel functions and the Legendre polynomials. Then, the energy lost from the incident wave due to scattering from the spherical scatterer is

$$E_{scattered} = 4\pi\rho_1\omega^3 \sum_{m=0}^{\infty} \frac{1}{2m+1}\left[\frac{1}{k_1}|A_m|^2 + \frac{m(m+1)}{K_1}|B_m|^2\right] , \qquad (77)$$

where A_m and B_m are the magnitudes of the scattered wave potentials and must be evaluated at the scattering surface by the boundary conditions.

The total energy of the wave is determined by calculating the energy in the incident plane wave that is being transported through a unit area normal to the propagation direction. The displacement of a plane compressional wave of unit amplitude traveling in the positive z-direction can be written as

$$\vec{u} = \hat{z}\, e^{i(\omega t - k_1 z)} . \qquad (78)$$

From elasticity theory, the stress can be calculated from the relation

$$\sigma_{ij} = \lambda(\nabla\cdot\vec{u})\,\delta_{ij} + \mu\left(\frac{\partial u_i}{\partial x_j} + \frac{\partial u_j}{\partial x_i}\right) , \qquad (79)$$

where

$$\delta_{ij} = \begin{cases} 1 & i=j \\ 0 & i\neq j \end{cases} .$$

For the wave described, $\sigma_{ij} = 0$ for all ij except

$$\sigma_{zz} = -\,i\,\frac{\rho_1}{k_1}\, e^{i(\omega t - k_1 z)} . \qquad (80)$$

The energy flux through a unit area is then given by

$$E_{inc} = \frac{i\omega}{2}\left\{(\sigma_{xz}u_x^* + \sigma_{yz}u_y^* + \sigma_{zz}u_z^*) - (\sigma_{xz}^*u_x + \sigma_{yz}^*u_y + \sigma_{zz}^*u_z)\right\} = \frac{\rho_1\omega^3}{k_1} . \qquad (81)$$

A similar calculation yields the energy flux for a plane shear wave to be

$$E_{inc} = \frac{\rho_i\omega^3}{K_1} . \qquad (82)$$

The scattering cross section is defined as

$$\gamma = \frac{E_{scattered}}{E_{total}} \quad . \tag{83}$$

The scattering cross section for a compressional plane wave encountering a spherical obstacle is then

$$\gamma_{shear} = 4\pi \sum_{m=0}^{\infty} \frac{1}{2m+1} \left[|A_m|^2 + m(m+1) \frac{k_1}{K_1} |B_m|^2 \right] \tag{84}$$

and that for a transverse plane wave is

$$\gamma_{comp} = 4\pi \sum_{m=0}^{\infty} \frac{1}{2m+1} \left[\frac{K_1}{k_1} |A_m|^2 + m(m+1) |B_m|^2 \right] . \tag{85}$$

If only spherical scatterers are present in the medium, Eqs. (84) and (85) can be substituted into Eq. (61) to determine the compressional and shear attenuation. Of course, before this can be accomplished the distribution function for the material must be known. Also, if other scatterer configurations are present, scattering cross sections for each type must be calculated using techniques similar to those above.

APPLICATION OF THE THEORIES TO SEA ICE

SCATTERING ATTENUATION APPROXIMATION

When sea ice freezes, the brine in the water concentrates in small pockets. The result is a system composed of frozen water with imbedded scattering centers filled with a brine fluid which is highly saline. Although these inclusions can have various geometries, the vast majority of those observed in annual sea ice by the authors of this report were spheroidal. This same situation may not necessarily hold for other types of sea ice, e.g., multi-year ice, but the acoustic and petrographic data necessary for evaluation of other types of sea ice are presently unavailable. Therefore, for the purposes of this calculation, it will be assumed that all of the scattering centers are brine-filled spheres.

Consider the application of the previous theory to the case of a plane wave being scattered from a liquid-filled sphere. The amplitudes of the scattered and transmitted waves are evaluated by solving the boundary conditions at the scattering surface for a wave striking a liquid-solid interface. By inserting Eqs. (67) through (69) into Eqs. (71a), (71c) and (71d) and evaluating at r = a, three simultaneous equations result. They are

$$I_{cm}[mj_m(k_1a) - k_1a\ j_{m+1}(k_1a) - I_{sm}[m(m+1)\ j_m(K_1a)]$$

$$= -A_m[mh_m(k_1a) - k_1ah_{m+1}(k_1a)] + B_m[m(m+1)\ h_m(K_1a)]$$

$$+ C_m\{mj_m(k_2a) - k_2a\ j_{m+1}(k_2a)] \quad , \tag{86a}$$

$$I_{cm}\left\{\left[m(1-m) + \frac{K_1^2a^2}{2}\right] j_m(k_1a) - 2k_1a\ j_{m+1}(k_1a)\right\}$$

$$+ I_{sm}[m(m+1)]\ [(m-1)\ j_m(K_1a) - K_1a\ j_{m+1}(K_1a)]$$

$$= -A_m\left\{\left[m(1-m) + \frac{K_1^2a^2}{2}\right] h_m(k_1a) - 2k_1a\ h_{m+1}(k_1a)\right\}$$

$$- B_m[m(m+1)]\ [(m-1)\ h_m(K_1a) - K_1a\ h_{m+1}(K_1a)]$$

$$+ \frac{\rho_2}{\rho_1}\frac{K_1^2a^2}{2} C_m\ j_m(k_2a) \quad , \tag{86b}$$

and

$$I_{cm}[(m-1)\ j_m(k_1a) - k_1a\ j_{m+1}(k_1a)]$$

$$+ I_{sm}\left[\left(1-m^2 + \frac{K_1^2a^2}{2}\right) j_m(K_1a) - K_1a\ j_{m+1}(K_1a)\right]$$

$$= -A_m[(m-1)\ h_m(k_1a) - k_1a\ h_{m+1}(k_1a)]$$

$$- B_m\left[\left(1-m^2 + \frac{K_1^2a^2}{2}\right) h_m(K_1a) - K_1a\ h_{m+1}(K_1a)\right] \quad . \tag{86c}$$

These three equations must be solved for the amplitudes A_m and B_m to evaluate the scattering cross section.

In Eq. (86), I_{cm} and I_{sm} are the amplitudes of the compressional wave and the shear incident wave, respectively. To consider the propagation of a shear wave in the medium, the amplitude of the compressional wave must vanish, i.e., $I_{cm} = 0$. It was shown earlier in Eq. (70) that I_{sm} is given by

$$I_{sm} = \frac{1}{K_1}(-i)^{m+1}(2m+1) \quad . \tag{87}$$

Using the values for the velocities and densities of annual sea ice from the experiment described in Appendix A and the computer program SCTTR given in Appendix B, we calculated the product of the scattering cross section and the frequency squared ($\gamma\nu^2$) vs the circumference-to-wavelength ratio of the scattering sphere. The results of this computation are shown in Figure 5. In the frequency region for which ka<<1, i.e., for wavelengths much larger than the scatterer radius, the scattering cross section is of the form

$$\gamma_{shear} \sim \nu^4 a^6 , \tag{88}$$

which is the result expected from standard Rayleigh[7] scattering. For frequencies such that ka>>1, the scattering cross section becomes of the form

$$\gamma_{\substack{shear \\ ka>10}} \sim \nu^{1.8} a^{3.8} . \tag{89}$$

In general, the shear wave scattering cross section for ka<1 and ka>15 can be approximated by

$$\gamma_{shear} \simeq \frac{\nu^4 a^6}{4.151 \times 10^{-9} + 2.35 \times 10^{-5} \nu^{2.2} a^{2.2}} \text{ dB/cm}^2 , \tag{90}$$

where the frequency (ν) is in MHz and the scatterer radius (a) is in cm. These expressions do not describe the erratic behavior of the scattering cross section where ka~1. The fluctuations in this region are due to bubble resonance and affect the cross section over a small ka span. However, for efficient propagation of the wave through the medium, frequencies with wavelengths approximately the same size as the scattering centers should be avoided.

For the case of a compressional wave incident on the bubble, $I_{sm} = 0$ and

$$I_{cm} = \frac{1}{k_1} (-i)^{m+1} (2m+1) . \tag{91}$$

The solution for the scattering cross section is determined following the same procedure described for the transverse wave. The results of this computation are also plotted in Figure 5 as a function of ka. For values of ka<1 and ka>15, the scattering cross section can be approximated by the equation

$$\gamma_{comp} \simeq \frac{\nu^4 a^6}{2.163 \times 10^{-7} + 0.017 \nu^4 a^4} \text{ dB/cm}^2 , \tag{92}$$

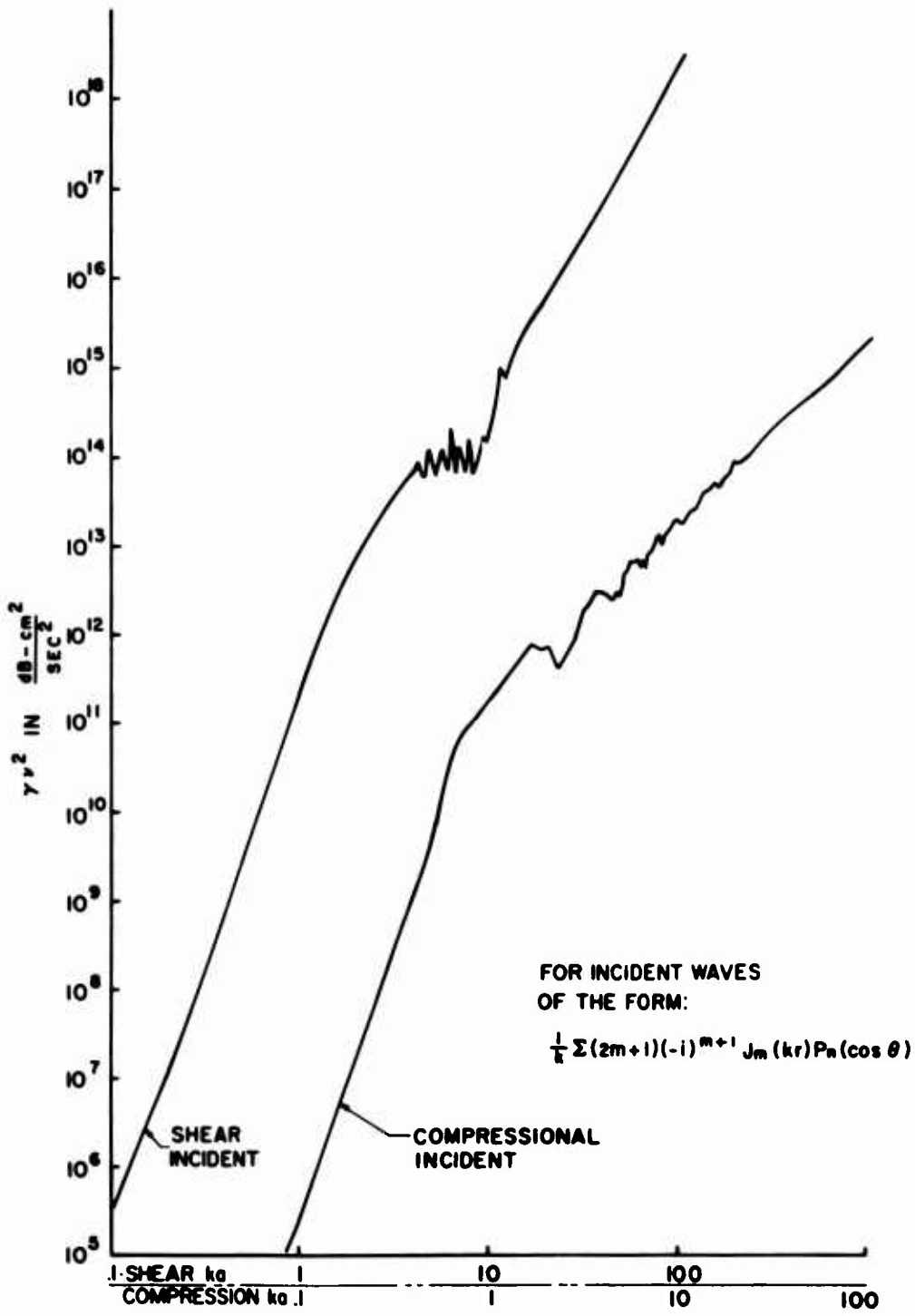

Figure 5. Results of Scattering Cross Section Calculation.

where ν is in MHz and a is in cm. As in the solution to the shear wave case, at low values of ka the compressional wave scattering cross section is dominated by Rayleigh scattering. For large values of ka, however, the cross section becomes a constant for the compressional wave while the transverse wave approaches infinity. This result indicates that when the wavelength becomes short the relative curvature of the scatterer becomes very large, so that the scattering problem approaches that of the transmission and reflection of an acoustic wave from a liquid layer in the ice medium. In this case, changes in frequency no longer affect the relative transmission of the compressional wave energy into the fluid, and the reflectivity, i.e., the scattered energy, remains constant. Conversely, if a shear wave strikes this boundary, it is totally reflected, i.e., the scattering cross section is infinite, because the fluid medium will not support shear waves.

To evaluate the attenuation due to scattering, the distribution functions in Eq. (61) must be either known or assumed. Because the necessary data are presently unavailable, and to minimize the complexity of the calculation, the following assumptions have been made.

(a) No interaction exists between the scattering centers, and the wave, once scattered, will not be re-scattered back into the sound beam. Since second order scattering should have only a small effect, particularly in the Rayleigh scattering region, this assumption should not greatly modify the calculation accuracy.

(b) There are N scattering centers per unit volume and the centers are uniformly distributed throughout the medium. From observations in the laboratory, this assumption appears to be relatively valid.

(c) All of the scattering centers are of the same size, with a radius a_o. This is probably an invalid assumption because it is known that a wide variety of brine pocket sizes is present in the medium. However, if radius a_o is selected as the average bubble size, then it can be argued that only the larger bubbles in the distribution will significantly affect the scattering. This assumption will make the calculated attenuation less than the actual attenuation that would be expected to occur during an experiment.

Using these assumptions, the attenuation due to scattering can be reduced to

$$\alpha_{\text{scattering}} = \frac{N}{2} \gamma(a_o) \quad , \tag{93}$$

which predicts the minimum attenuation to be expected from this mechanism.

Laboratory measurements of void size and concentration yield radii on the order of 0.065 cm and concentrations on the order of 25 holes per cm^3. Using the curves of Figure 5 and the relation

$$ka = \frac{2\pi\nu}{c} a \quad , \tag{94}$$

where ν is the frequency in Hz, c is the velocity in cm/sec, and a is the radius in cm, the attenuation due to scattering at 500 kHz is calculated as

$$\alpha_{\text{scattering comp}} = 25 \text{ dB/meter}$$

and

$$\alpha_{\text{scattering shear}} = 350 \text{ dB/meter} \; . \tag{95}$$

At 100 kHz

$$\alpha_{\text{scattering comp}} = 0.045 \text{ dB/meter}$$

and

$$\alpha_{\text{scattering shear}} = 2.25 \text{ dB/meter} \; . \tag{96}$$

In general, for ka<1 and ka>15

$$\alpha_{\text{shear}} \simeq \frac{\nu^4}{4.403 \times 10^{-5} + 6.097 \times 10^{-4}\, \nu^{2.2}} \text{ dB/m}$$

and (97)

$$\alpha_{\text{comp}} \simeq \frac{\nu^4}{2.294 \times 10^{-3} + 3.253 \times 10^{-3}\, \nu^4} \text{ dB/m} \quad ,$$

where ν is in MHz. For values of 1<ka<15, the approximations of Eq. (92) are still more or less valid for order of magnitude calculations, but will invariably yield predictions which are significantly low.

TOTAL ATTENUATION APPROXIMATION

As was discussed in the introduction, the attenuation in sea ice is composed of two parts,

$$\alpha = \alpha_{\text{classical}} + \alpha_{\text{scattering}} \; . \tag{98}$$

Before the total attenuation can be estimated, the classical attenuation must be considered. The experiment outlined in Appendix A gives the results necessary for an approximation to the solution of the two-element classical models. During this experiment, the total attenuation and velocity were measured in situ 15 cm below the surface in annual sea ice. At 100 kHz, the results of these measurements gave a longitudinal wave velocity of 3790 m/sec, a shear wave velocity of

1923 m/sec, a density of 0.937 g/cm^3, and a generalized attenuation of 0.18 dB/cm. Using these values, and assuming the elastic and viscous constants to be frequency independent, we solved both the Voigt and the Maxwell model as a function of frequency. The results are shown in Figure 6, along with the scattering attenuation. From this representation it can be concluded that, for frequencies above approximately 5 kHz, the Maxwell model fails because, from the physics of the problem, there is no frequency region over which the attenuation remains constant. For frequencies lower than 1 MHz, these curves show that both the attenuation predicted by the Voigt model and that predicted by the scattering calculations can be found by utilizing their low frequency approximations. Thus, if it is assumed that the total attenuation is the sum of the results of the Voigt model and the scattering calculations, then the attenuation will increase as ν^2 for frequencies below approximately 250 kHz and as ν^4 for higher frequencies because of the dominance of the scattering contribution. The total attenuation curve for the shear wave is shown in Figure 7.

DEPTH DEPENDENCE OF SHEAR WAVE PROPAGATION

Recent experimental data[8] have demonstrated that for annual sea ice the velocity of longitudinal waves exhibits dependence on the depth into the medium because of variations in density, salinity and temperature. It is reasonable to assume that these same parameters will similarly affect the propagation of the shear wave. Therefore, it is desirable to prognosticate the form of the depth dependence. To accomplish this calculation, it is assumed that the measurement frequency is sufficient to ignore the viscous terms in the propagation equation, or, equivalently, that the viscous terms do not greatly affect the velocity. Thus, a near-elastic medium is assumed, for which, according to elasticity theory, the longitudinal and transverse wave velocities are given by

$$C_L = \sqrt{\frac{E}{\rho}\frac{(1-\epsilon)}{(1+\epsilon)(1-2\epsilon)}} = \sqrt{\frac{\lambda+2\mu}{\rho}}$$

$$C_T = \sqrt{\frac{E}{\rho}\frac{1}{2(1+\epsilon)}} = \sqrt{\frac{\mu}{\rho}} \quad , \tag{99}$$

where

C_L is the velocity of the longitudinal wave
C_T is the velocity of the shear wave
ϵ is Poisson's ratio
E is Young's modulus
μ is the shear modulus
λ is the Lame´ constant
ρ is the density.

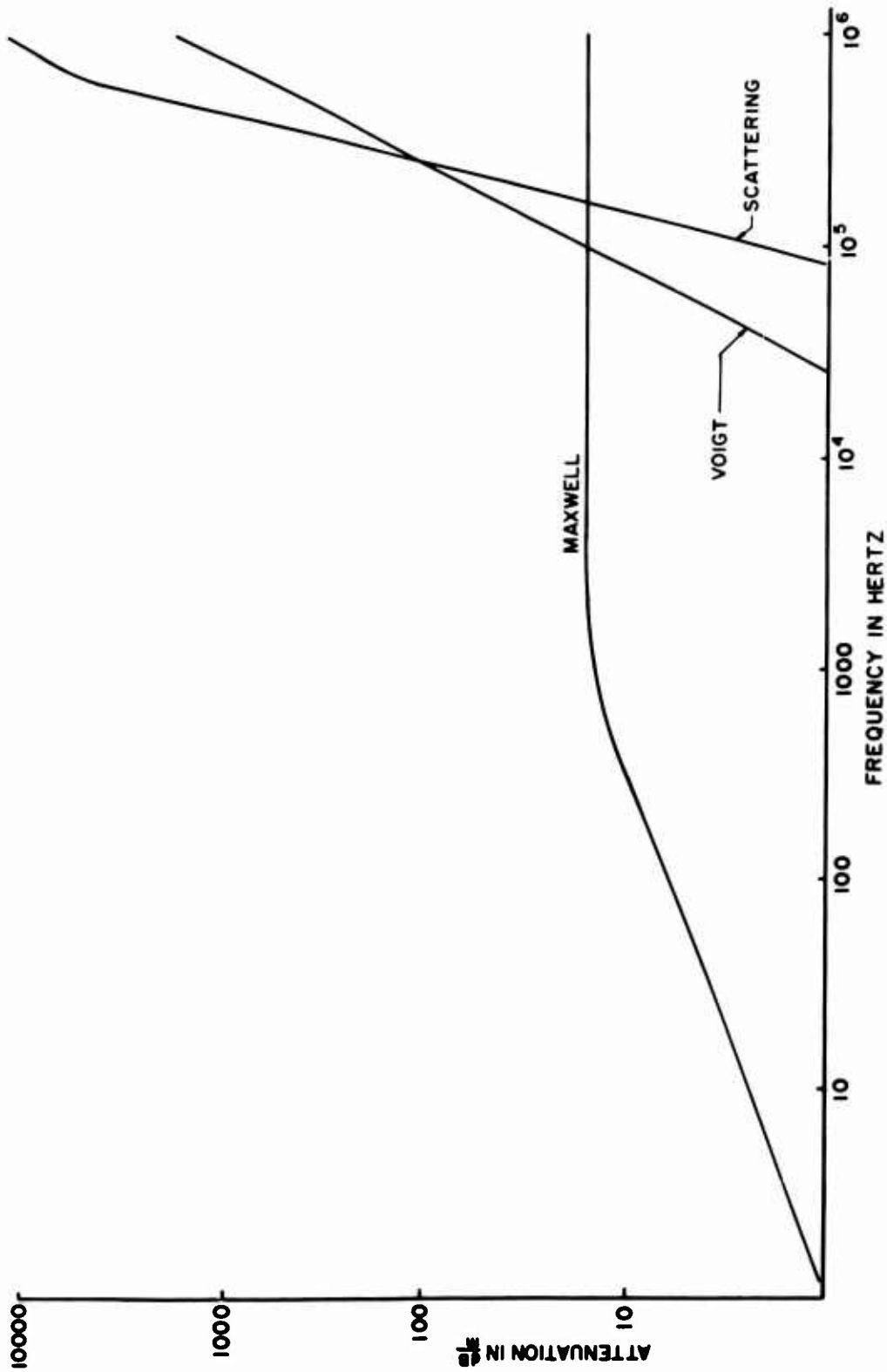

Figure 6. Attenuation Contributions of the Maxwell Model, the Voigt Model and Scattering.

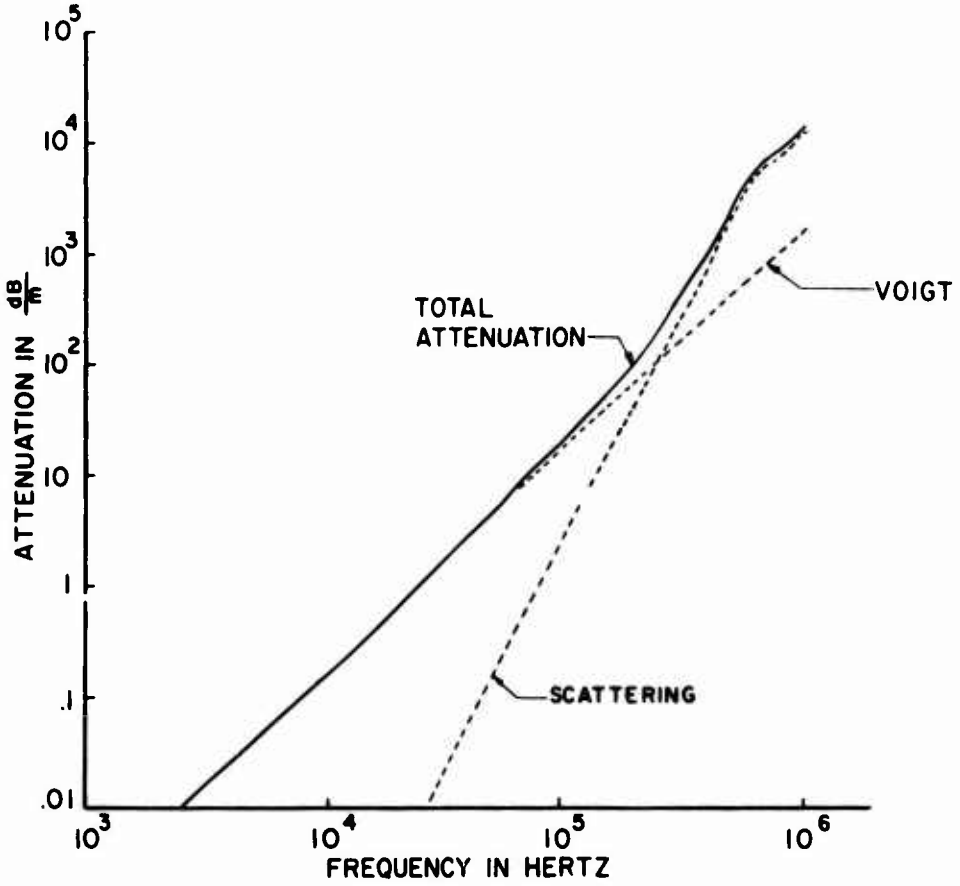

Figure 7. Predicted Attenuation in Annual Sea Ice.

Langleben[9] has empirically related Young's modulus of sea ice to the brine content (ν) by the equation

$$E = (10.0 - 35.1\ \nu) \times 10^{10}\ \text{dyne/cm}^2 \ . \qquad (100)$$

The brine content in this equation can be determined from the salinity (S) and the temperature (θ) by the relations[10]

$$\nu = S\left(\frac{52.56}{\theta} - 2.28\right) \quad -0.5° \leq \theta \leq -2.6°$$

$$\nu = S\left(\frac{45.917}{\theta} + 0.930\right) \quad -2.6° \leq \theta \leq -8.2° \ , \qquad (101)$$

$$\nu = S\left(\frac{45.795}{\theta} + 1.189\right) \quad -8.2° \leq \theta \leq -27.9°$$

where

S is the salinity in parts per thousand
ν is the brine content in parts per thousand
θ is the absolute value of the temperature in °C.

Using these equations and the data in Ref. 8, the depth dependence of the shear wave velocity has been calculated and is shown in Figure 8. The calculation shows that the shear wave velocity decreases continuously with depth and may approach zero at the ice-water interface (a depth of 145 cm for this experiment). This decrease in velocity can be related to the vertical distribution of the liquid brine present in the ice cover. The result, then, indicates that the boundary might not provide a good reflecting surface for the transverse acoustic mode.

Unfortunately, sufficient data do not exist to similarly predict the depth dependence for attenuation. For this determination, the form of both the elastic and viscous coefficients must be known. However, if a near-elastic medium is assumed, it can be shown that for a Voigt solid

$$\tau \sim \frac{\rho \eta \omega^2}{2C^3} \quad . \tag{102}$$

Therefore, provided the depth dependence of the viscosity (η) does not decrease faster than C^3, the attenuation will become infinite as the shear velocity goes to zero at the boundary.

CONCLUSIONS

The attenuation of an acoustic wave in any material is a result of the combination of classical dissipation and scattering effects. For sea ice it was shown that the Maxwell model for classical attenuation does not apply to the dynamic case because it predicts constant attenuation at frequencies above a few kHz. This conclusion probably can be extended to more complex models that have Maxwell elements in series because it was shown that whenever this component is in that position it dominates the model. Therefore, if more complex models are required to predict experimental values using frequency independent parameters, combinations of Voigt and Maxwell elements in parallel will be required.

A minimum attenuation due to scattering was derived by solving for the scattering cross section of a single liquid-filled spherical scatterer, assuming a uniform bubble population and size. It was shown that for the frequencies of interest, Rayleigh scattering predominates where the attenuation is predicted to be proportional to the fourth power of the frequency. Assuming a dissipation that could be predicted by a single Voigt

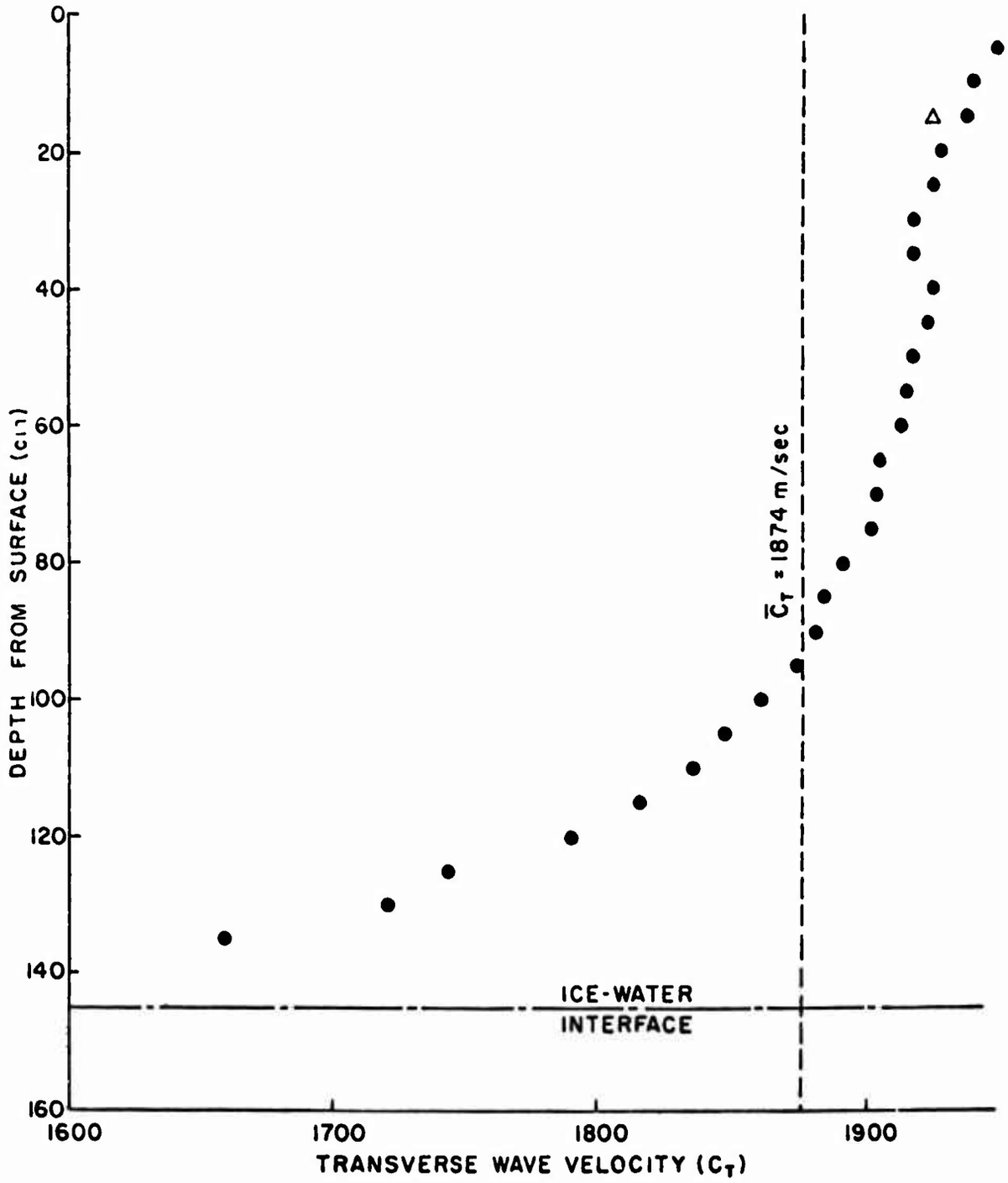

Figure 8. Depth Dependence of the Shear Wave Velocity.

element, we derived a frequency-dependent curve composed of the attenuation predicted from both classical and scattering sources. This calculation was based on measured values of sea ice velocity and attenuation at 100 kHz. The results indicate that for frequencies above 250 kHz scattering dominates, and the attenuation for the shear wave will be in excess of 100 dB/meter.

Therefore, based upon these predictions, all experiments for which an acoustic shear wave is to be used and for which penetration into the medium is desired (such as sea-ice thickness measurements) should use frequencies of 20 kHz or lower depending upon the distance the sound wave is expected to travel. For velocities on the order of 2000 m/sec, these frequencies will have wavelengths of 10 cm or longer. At these wavelengths, resolution is very poor.

The probability that attenuation is a continuously varying parameter depending on the distance from the ice surface was discussed. Insufficient experimental data presently exist to verify or deny this assumption. However, since the temperature of sea ice varies with the depth from the surface, higher concentrations of liquid brine could result which would contribute to a decrease in shear wave velocity and an increase in the expected attenuation.

APPENDIX A

DESCRIPTION OF IN SITU SHEAR WAVE EXPERIMENT

During March 1973, an extensive experiment was performed in the Chukchi Sea near Pt. Barrow, Alaska, to determine the acoustic propagation characteristics of annual sea ice. Although these experiments succeeded in measuring compressional velocity profiles for the first time, similar profiles for the shear wave were not obtained. The principal difficulty in making shear wave measurements is obtaining a reliable bond between the medium and the shear wave generating transducers. This difficulty is largely due to the "leaching" of the brine, which generates a highly saline liquid surface layer.

Washing the bonding surface with fresh water has been partially successful in both laboratory and in situ tests. The experiment shown in Figure A1 was attempted during the field tests discussed above. Channels were cut in the ice canopy to a depth of ~45 cm, and located a known distance apart. The sides of the channel were washed with fresh water to eliminate the saline boundary layer and shear-sensitive transducers were quickly coupled to the ice at a depth of 15 cm on diametrically opposite sides of the test section. The electronics consisted of a pulse timing generator which furnished PRF and pulse length information to a pulsed power oscillator and a trigger signal to the oscilloscope. The oscillator, in turn, provided a cw pulse of the desired frequency, pulse length and pulse rate to the transmitting transducer coupled to the ice. The transmitted acoustic signal was received by the receiving transducer coupled to the opposite side of the test section, amplified and transmitted to the oscilloscope. The time of flight of the acoustic pulse in the test section was determined by measuring the oscilloscope sweep time from the origin to the first received signal by means of a calibrated time delay and then correcting for electronic time losses. Thus, knowing the specimen length, the velocity could be calculated. This method is accurate to approximately 1-1/2%, depending on how precisely the length of the sample is known.

This technique was used in a series of measurements during which the test section was incrementally decreased and the process repeated. These measurements yielded an average attenuation of 18 dB/meter and an average velocity of 1923 m/sec at 100 kHz. The velocity is shown as an experimental point in Figure 8. Further laboratory measurements of shear wave velocity on sea ice samples using techniques similar to those of the in situ experiment showed an average velocity of 1870 m/sec, which agrees very well with the average predicted profile velocity of 1874 m/sec.

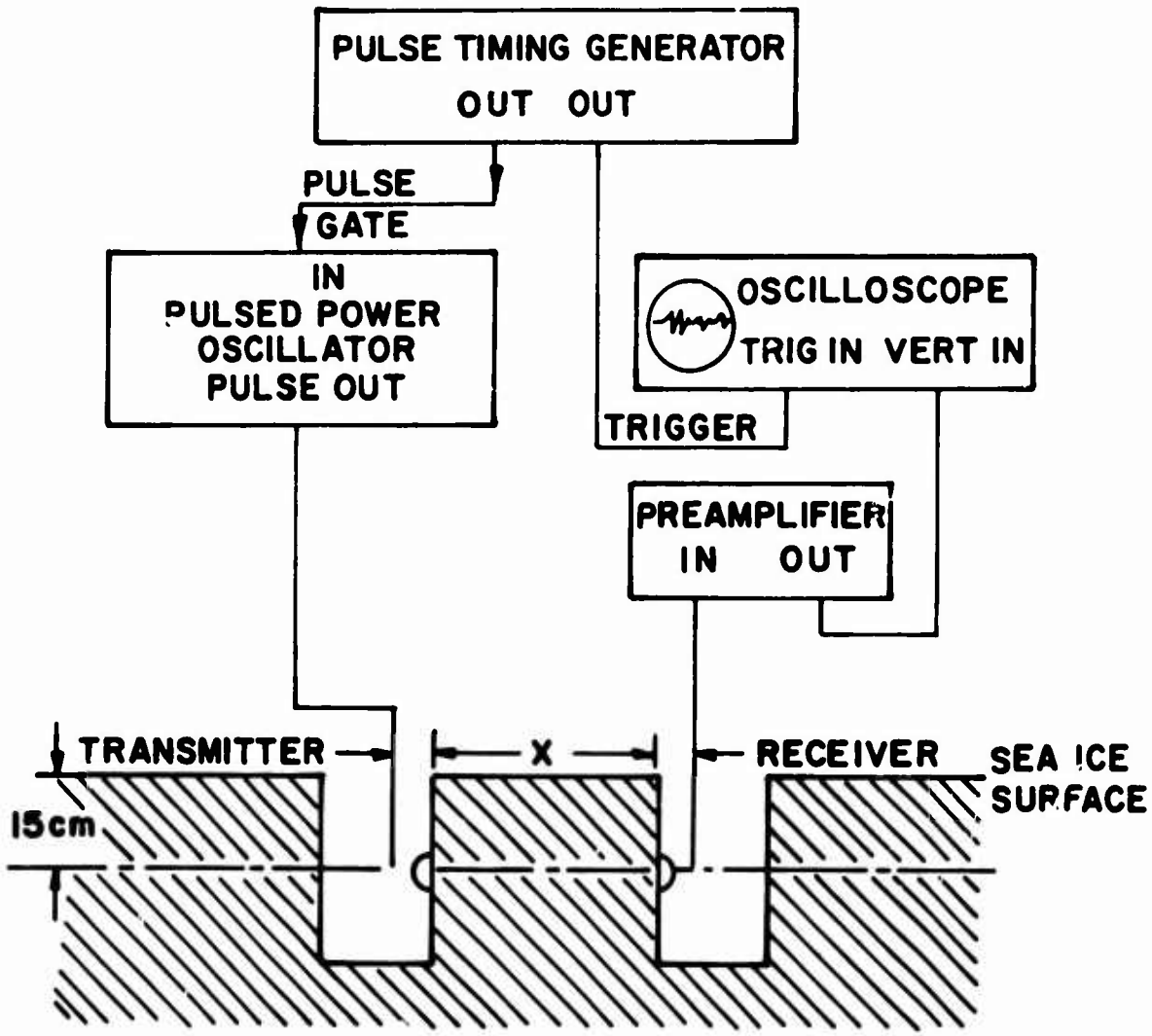

Figure A1. Diagram of the In Situ Experiment.

APPENDIX B

COMPUTER PROGRAMS

```
      PROGRAM SSCTR(INPUT,OUTPUT,TAPE5=INPUT,TAPE6=OUTPUT)
C     THIS PROGRAM CALCULATES THE SCATTERING CROSS SECTION TIMES THE
C     FREQUENCY SQUARED.  THE VALUE IS CALCULATED FOR A SHEAR PLANE
C     WAVE IN A SOLID STRIKING A FLUID FILLED SPHERE.  THE CASE OF A
C     COMPRESSIONAL WAVE STRIKING THE SPHERE IS ALSO CALCULATED.  THE
C     VALUE IS CALCULATED AS A FUNCTION OF THE DIMENSIONLESS PARAMETER
C     KA WHERE K=2*PI*FREQ/VELOCITY AND A IS THE SPHERE RADIUS.
C     THE CALCULATION IS MADE IN THE C.G.S.SYSTEM.  THE SCATTERING
C     CROSS SECTION HAS UNITS OF DB-CM**2.  CS1 IS THE SHEAR VELOCITY
C     AND CL1 IS THE COMPRESSIONAL VELOCITY IN THE SOLID.  CL2 IS THE
C     COMPRESSIONAL VELOCITY IN THE SCATTERER.  RHO IS THE RATIO OF THE
C     DENSITY OF THE SPHERE TO THE DENSITY OF THE SOLID.
      READ(5,49) CS1,CL1,CL2,RHO
   49 FORMAT(3F8.0,F6.3)
      WRITE(6,51)
   51 FORMAT(42H      KA        GAMMA,SHEAR        GAMMA,COMP)
    1 READ(5,50) AKA
   50 FORMAT(F7.2)
      IF(EOF,5) 7,8
    8 CONTINUE
      PI=3.141592654
C     FIRST THE SHEAR SCATTERING IS CALCULATED.
      BKS1=AKA
      BKL1=BKS1*CS1/CL1
      BKL2=BKS1*CS1/CL2
      SIM=CS1/(2.*PI)
C     IF CIM=0. THEN A SHEAR WAVE IS INCIDENT.
      CIM=0.
      CALL COEF(BKS1,BKL1,BKL2,SIM,CIM,RHO,GAMAS)
      GAMAS=GAMAS*BKS1
C     GAMAS IS THE SHEAR SCATTERING CROSS SECTION*FREQ**2.
C     NOW THE COMPRESSIONAL SCATTERING IS CALCULATED.
      BKL1=AKA
      BKS1=BKL1*CL1/CS1
      BKL2=BKL1*CL1/CL2
C     IF SIM=0. THEN A COMPRESSIONAL WAVE IS INCIDENT.
      SIM=0.
      CIM=CL1/(2.*PI)
      CALL COEF(BKS1,BKL1,BKL2,SIM,CIM,RHO,GAMAC)
      GAMAC=GAMAC*BKL1
C     GAMAC IS THE COMPRESSIONAL SCATTERING CROSS SECTION*FREQ**2.
      WRITE(6,55) AKA,GAMAS,GAMAC
   55 FORMAT(2XF7.2,2(5XE13.4))
      GO TO 1
    7 CONTINUE
      END
```

```
      SUBROUTINE COEF(AKS1,AKL1,AKL2,SI,CI,RHA,GAMMA)
      DIMENSION AJ1(400), AJ2(400), AJ3(400), Y1(400), Y2(400)
C     THIS SOLVES THE BOUNDARY CONDITIONS FOR THE AMPLITUDES OF THE
C     SCATTERED WAVES.  THE AMPLITUDES ARE USED TO CALCULATE THE
C     SCATTERING CROSS SECTION.
      CALL SPBES(AKS1,N1,AJ1)
      CALL SPBES(AKL1,N2,AJ2)
      CALL SPBES(AKL2,N3,AJ3)
      PI=3.141592654
      IF(N1-N2) 10,11,11
   10 N=N2
      GO TO 12
   11 N=N1
   12 IF(N-N3) 13,14,14
   13 NM=N3
      GO TO 15
   14 NM=N
C     NM IS THE UPPER LIMIT OF THE SUM IN THE SCATTERING CROSS SECTION.
   15 CALL SNMN(AKS1,NM,Y1)
      CALL SNMN(AKL1,NM,Y2)
      GAMMA=0.
      DO 100 M=1,NM
      F=FLOAT(M)-1.
      ZERO=0.
      D11=F*AJ2(M)-AKL1*AJ2(M+1)
      D12=ZERO-F*(F+1.)*AJ1(M)
      RAT=F*(1.-F)+AKS1**2/2.
      D21=RAT*AJ2(M)-2.*AKL1*AJ2(M+1)
      D22=F*(F+1.)*((F-1.)*AJ1(M)-AKS1*AJ1(M+1))
      D31=(F-1.)*AJ2(M)-AKL1*AJ2(M+1)
      ROT=1.-F**2+AKS1**2/2.
      D32=ROT*AJ1(M)-AKS1*AJ1(M+1)
      CI11=F*Y2(M)-AKL1*Y2(M+1)
      CI12=F*(F+1.)*Y1(M)
      C13=F*AJ3(M)-AKL2*AJ3(M+1)
      CI21=RAT*Y2(M)-2.*AKL1*Y2(M+1)
      CI22=F*(F+1.)*((F-1.)*Y1(M)-AKS1*Y1(M+1))
      C23=RHA*AKS1**2*AJ3(M)/2.
      CI31=(F-1.)*Y2(M)-AKL1*Y2(M+1)
      CI32= ROT*Y1(M)-AKS1*Y1(M+1)
      Z1=(D11*CI+D12*SI)
      Z2=(D21*CI+D22*SI)
      Z3=(D31*CI+D32*SI)
      ARM=D22*C13*Z3+C23*D32*Z1-C23*Z3*D12-D32*Z2*C13
      AIM=C13*CI22*Z3+C23*CI32*Z1+C23*Z3*CI12-CI32*Z2*C13
      BRM=D31*Z2*C13+C23*Z3*D11-C13*Z3*D21-C23*Z1*D31
      BIM=C13*Z2*CI31+C23*Z3*CI11-C13*Z3*CI21-C23*Z1*CI31
      DRM=C23*(D12*D31+CI12*CI31-D11*D32+CI11*CI32)+C13*(D21*D32-CI21*
     1CI32-C22*D31+CI22*CI31)
      DIM=C23*(CI31*D12-CI12*D31-CI11*D32-CI32*D11)+C13*(D32*CI21+D21*
     1CI32-CI22*D31-D22*CI31)
      P=ARM/DRM
      Q=BRM/DRM
```

```
      R=DIM/DRM
      S=AIM/DRM
      T=BIM/DRM
      DEN=1.+R**2
C     AM AND BM ARE THE SQUARES OF THE MAGNITUDE OF THE SCATTERED WAVES.
      AM=(P**2+S**2)/DEN
      BM=(Q**2+T**2)/DEN
      GP=(2.*F+1.)*4.*PI*(AM/AKL1+F*(F+1.)*BM/AKS1)
      GAMMA=GAMMA+GP
  100 CONTINUE
      GAMMA=8.686*GAMMA
      RETURN
      END
```

```
      SUBROUTINE SNMN(ZT,NN,Y)
      DIMENSION Y(400)
C     THIS CALCULATES THE SPHERICAL NEUMANN FUNCTION(Y(I)) OF ARG ZT AND
C     UP TO ORDER NN.  THE VALUES ARE CALCULATED BY UPWARD RECURSION
C     RELATIONS.
      ZERO=0.
      DO 1 I=1,400
    1 Y(I)=0.
      Y(1)=ZERO-COS(ZT)/ZT
      Y(2)=ZERO-COS(ZT)/ZT**2-SIN(ZT)/ZT
      NT=NN+2
      DO 2 I=3,NT
      AJ=FLOAT(I)-2.
      Y(I)=((2.*AJ+1.)/ZT)*Y(I-1)-Y(I-2)
    2 CONTINUE
      RETURN
      END
```

```
      SUBROUTINE SPBES(ZT,NT,AJ)
      DIMENSION R(400), RJ(400), AJ(400)
C     THIS CALCULATES THE SPHERICAL BESSELS FUNCTIONS(AJ(I)) OF ARG
C     ZT UP TO ORDER NT.
C     THIS ROUTINE IS VALID FOR ARGUMENTS AS LOW AS 0.05.
      BT=ZT
      NDIM=400
      NZT=IFIX(ZT)
      DO 100 I=1,NDIM
  100 AJ(I)=0.
C     THIS SECTION SETS THE UPPER LIMIT OF NT FOR THE GIVEN ARG SUCH
C     THAT ALL AJ#S OF HIGHER ORDER CAN BE SET TO ZERO.
      N=NZT+10
      DO 1 I=N,1850,5
```

```
      J=I
      FI=FLOAT(I)
      SECA=ZT/(FI+.5)
      TACA=SQRT(1.-SECA**2)
      COSA=1./SECA
      SINA=SQRT(1.+COSA**2)
      ALP=ALOG(COSA+SQRT(COSA**2-1.))
      DELT=EXP((FI+.5)*(TACA-ALP))/(2.*(FI+.5)*SQRT(SINA))
      IF (DELT-1.E-27) 5,5,1
    1 CONTINUE
      GO TO 12
    5 N=J
      FN=FLOAT(N)
      NP=N+1
      NT=N+2
      NU=N+10
      EXPR=EXP(1.)
      DO 7 I=NU,1000,5
      K=I
      FI=FLOAT(I)
      D=0.434294
      A1=2.*(FI-FN+1.)*D*ALOG(ZT)
      A2=(2.*FI-2.*FN+1.)*D*ALOG(EXPR)
      A3=(FN+2.5)*D*ALOG(FN+2.)+(FN-1.5)*D*ALOG(FN-2.)
      A4=(FI+3.5)*D*ALOG(FI+3.)
      A5=(FI-.5)*D*ALOG(FI-1.)
      E=A1+A2+A3-A4-A5
      IF(E+10.) 9,9,7
    7 CONTINUE
C     THIS SECTION CALCULATES THE BESSEL FUNCTIONS.
      GO TO 12
    9 NU=K
      J=NU
      R(NU+1)=0.
      DO 2 I=1,NU
      K=I
      SJ=FLOAT(J)
      R(J)=ZT/(1.+2.*SJ-ZT*R(J+1))
      IF(R(J)-1.) 2,2,8
    2 J=J-1
      GO TO 200
    8 IF(J-2) 200,200,14
  200 RJ(NU+1)=R(NU)
      RJ(NU)=1.
      J=NU
      NUP=NU-1
      DO 210 I=1,NUP
      J=J-1
      SJ=FLOAT(J)
      RJ(J)=(1.+2.*SJ)/ZT*RJ(J+1)-RJ(J+2)
  210 CONTINUE
      ALPH=(RJ(1)-ZT*RJ(2))*COS(BT)+ZT*SIN(BT)*RJ(1)
      DO 220 I=1,NT
```

```
220 AJ(I)=RJ(I)/ALPH
333 CONTINUE
    RETURN
 14 RJ(J+1)=R(J)
    LAM2=J+2
    IF(LAM2-NP) 15,44,44
 15 RJ(J)=1.
    J=J-1
    K=K+1
    DO 3 I=K,NU
    SJ= FLOAT(J)
    RJ(J)=(1.+2.*SJ)/ZT*RJ(J+1)-RJ(J+2)
  3 J=J-1
    DO 4 I=LAM2,NT
  4 RJ(I)=RJ(I-1)*R(I-1)
    ALPH=(RJ(1)-ZT*RJ(2))*COS(BT)+ZT*SIN(BT)*RJ(1)
    NDM=NDIM-1
    IF(NT-NDM) 16,16,17
 17 NT=NDM
 16 DO 6 I=1,NT
  6 AJ(I)=RJ(I)/ALPH
105 CONTINUE
    RETURN
 44 WRITE(6,45)
 45 FORMAT(25H LAMBDA+2.GE.N+1  END XEQ)
    GO TO 105
 12 WRITE(6,13) ZT
 13 FORMAT(26H ARG BES FTN TOO LARGE ZT=,E20.8,5X14H END EXECUTION)
    STOP
    END
```

REFERENCES

1. W. Weeks and A. Assur, "The Mechanical Properties of Sea Ice," Cold Regions Research and Engineering Laboratory Report (1967).

2. C. Maxwell, Scientific Papers (Cambridge University Press, 1890).

3. W. Voigt, Ann. d. Phys. 47, 671 (1892).

4. H. Love, The Mathematical Theory of Elasticity (Cambridge University Press, New York, 1927).

5. P. M. Morse and H. Feshbach, Methods of Theoretical Physics, (McGraw-Hill Publishing Co., New York, 1953).

6. C. F. Ying and Rohn Truell, "Scattering of a Plane Longitudinal Wave by a Spherical Obstacle in an Isotropically Elastic Solid," J. Appl. Phys. 27, 1086-1096 (1956).

7. Lord Rayleigh, Theory of Sound (Dover Publications, 1945).

8. R. E. Bunney and J. G. Hanse, "Acoustic Velocity Profiles in Annual Sea Ice," (manuscript submitted to J. Acoust. Soc. Am. for publication).

9. M. P. Langleben, "Young's Modulus for Sea Ice," Can. J. Phys. 40, 1-8 (1962).

10. G. Frankenstein and R. Garner, "Equations for Determining the Brine Volume of Sea Ice From -0.5°C to -22.9°C," J. Glaciology 6, 943-944 (1967).

*U.S. GOVERNMENT PRINTING OFFICE: 1974—A-0004/32